to be submitted to Atomization and Sprays, 30(x):1–29 (2020)

REEVALUATING THE JET BREAKUP REGIME DIAGRAM

Ben Trettel*

Trettel Research LLC, Jefferson, MD 21755, USA

*Address all correspondence to: Ben Trettel,
E-mail: http://trettelresearch.com/contact.html

Original Manuscript Submitted: mm/dd/2019; Final Draft Received: mm/dd/2020

Identifying the regime of a liquid jet is necessary to determine the physical mechanisms causing breakup and consequently how to model the jet. Existing regime diagrams are based on a small amount of data classified by superficial visual characteristics, making these diagrams too inaccurate to reliably determine the correct regime. A more accurate regime diagram is developed using a large compilation of breakup length data combined with theory where the data is sparse. Improvements in the regime diagram include a new regime, the addition of the nozzle critical Reynolds number and the turbulence intensity as variables, and the recognition that how the regimes change with increasing velocity (i.e., Rayleigh to first wind-induced to second wind-induced to atomization) is not universal.

KEY WORDS: *liquid jet breakup, regimes, turbulence intensity, dripping, Rayleigh regime, first wind-induced, second wind-induced, atomization, turbulence transition*

1. INTRODUCTION

Liquid jets break up through many mechanisms, and most mechanisms must be modeled differently. Even focusing solely on the case of the breakup of Newtonian jets injected into still low density environments without consideration of cavitation, Mach number effects, or evaporation, there are many varieties of jet breakup. Which "regime" a jet is in depends on factors including but not limited to the Reynolds number, Weber number, the liquid-gas density ratio, and the turbulence intensity.

Accurately determining the regime is necessary for both research on and design of systems in liquid jet breakup. Engineers often apply models applicable only in a particular regime to an inappropriate regime. Researchers may decide they want to study a particular regime, and consult a regime diagram to determine where to place their study. Frequently, the study is placed in a regime different from that intended. Researchers have also highlighted so-called contradictions between previous studies, when in fact there are no contradictions, and the studies were in different regimes than believed.

Conventionally, the regime of a liquid jet has been determined through subjective comparison of the appearance of the jet against prototypical jet photographs in the literature, e.g., Lin and Reitz (1998, fig. 1). Classification of photographs has also been used to produce *regime diagrams* which allow determination of the regime given variables like the jet Reynolds and

Ohnesorge numbers. Unfortunately several regimes appear superficially similar (e.g., the "second wind-induced" and "atomization" regimes), despite differing in terms of more objective characteristics like the trend in the breakup length curve, as will be discussed. This causes photographic classification to frequently be inaccurate, also drawing into question regime diagrams based on photographs. For this reason, objective characteristics are preferred when classifying regimes.

Regime diagrams are also typically constructed from relatively little data, lacking the resolution needed to precisely determine the boundaries of each regime. This problem is avoided in this work through a large data compilation I developed Trettel (2020a,b). Additionally, this data compilation specifically included only data with known turbulence intensity, as the influence of this variable on jet breakup (including but not limited to the regime diagram) is typically only hypothesized, and rarely validated against experimental data with appreciable turbulence intensity variation.

In this paper I'll first discuss the most popular regime diagram as of this writing (figure 3), then detail problems with this regime diagram. I will conclude with a largely new regime diagram (figure 4) which is much more accurate than any previous diagram for the cases of interest in this work.

The notation used in this work is identical to that of my other jet breakup work (Trettel, 2020a). The nozzle outlet is specified with the subscript 0, e.g., the jet's bulk velocity is $\overline{U}_0$ and d_0 is the nozzle outlet diameter. The subscript ℓ refers to liquid properties, e.g., ρ_ℓ is the liquid density. Similarly, the subscript g refers to gas properties, e.g., ρ_g is the gas density. The liquid phase Weber number $\mathrm{We}_{\ell 0} \equiv \rho_\ell \overline{U}_0^2 d_0/\sigma$ where σ is the surface tension of the liquid. A gas phase Weber number can be defined as $\mathrm{We}_{\mathrm{g}0} \equiv \rho_\mathrm{g} \overline{U}_0^2 d_0/\sigma$. The liquid phase Reynolds number is $\mathrm{Re}_{\ell 0} \equiv \overline{U}_0 d_0/\nu_\ell$ where ν_ℓ is the liquid kinematic viscosity. The plane-averaged turbulent kinetic energy at the nozzle outlet (analogous to the bulk velocity) is $\overline{k}_0$. Using the turbulent kinetic energy, the turbulence intensity can be defined as $\overline{\mathrm{Tu}}_0 \equiv \left(2\overline{k}_0/3\right)^{1/2}/\overline{U}_0$. The motivation behind this particular definition of the turbulence intensity is described by Trettel (2020a,b).

There are multiple quantities of interest in jet breakup, however, this work focuses most heavily on the (average) breakup length $\langle x_\mathrm{b} \rangle$, a measure of the droplet size like the Sauter mean diameter D_{32}, and to a lesser extent the (average) breakup onset location $\langle x_\mathrm{i} \rangle$. The breakup length and breakup onset location are shown schematically in figure 1. The breakup length is defined as the average distance from the nozzle outlet to where the core of the jet ends. Similarly, the breakup onset location is defined as the average distance from the nozzle outlet to where breakup first starts.

2. PREVIOUS REGIME DIAGRAMS

The conventional regimes are (Birouk and Lekic, 2009; Lefebvre and McDonell, 2017; and Lin and Reitz, 1998):

1. Dripping regime — The jet velocity is so low that breakup is driven by gravity, producing relatively large droplets.

2. Rayleigh regime — Breakup due to a surface-tension-driven instability resulting in droplets larger than the nozzle outlet diameter but of the same order of magnitude ($D \approx 1.89 d_0$). The breakup length $\langle x_\mathrm{b} \rangle$ is increasing with increasing jet velocity.

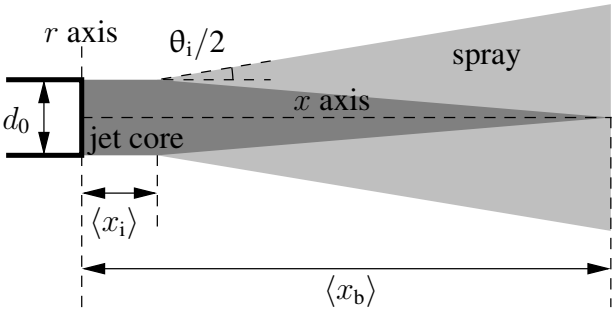

FIG. 1: Jet breakup variables labeled on a schematic liquid jet. d_0 is the nozzle outlet diameter, $\langle x_i \rangle$ is the average breakup onset location, θ_i is the spray angle, and $\langle x_b \rangle$ is the breakup length.

3. First wind-induced regime — Convention states that the droplet diameters are on the order of the nozzle outlet diameter (Lin and Reitz, 1998, fig. 1), however, I challenge this view later in this chapter. Similarly, the breakup onset location is conventionally stated as many diameters from the orifice, but this is not necessarily true either. However, previous researchers did correctly understand that the breakup length $\langle x_b \rangle$ is decreasing with increasing jet velocity in this regime (Reitz, 1978, p. 165, fig. 1.1).

4. Second wind-induced regime — The droplet diameters are smaller than the nozzle outlet diameter. The average breakup onset location is not negligible, but can be small. The breakup length $\langle x_b \rangle$ is increasing in a power law with increasing jet velocity.

5. Atomization regime — Droplet sizes are much smaller than the nozzle outlet diameter. Defined frequently as breakup starting at the nozzle outlet (e.g., $\langle x_i \rangle = 0$), though this is probably not true as will be discussed. In this work I instead suggest that $\langle x_i \rangle$ is small. In the absence of cavitation and Mach number effects, the breakup length $\langle x_b \rangle$ plateaus as the jet velocity is increased.

These regime names have slowly evolved since the early works of Haenlein (1932) and von Ohnesorge (2019). As previously mentioned, the regimes also have been defined mainly in two different ways: one is subjective evaluation of photographs of jets, another is more objective, based instead on measurements of quantities like the breakup length, $\langle x_b \rangle$. Details of the problems with subjective definitions will be discussed in § 3.7. Unfortunately the subjective and objective approaches have not always been unified. For example, Lefebvre and McDonell (2017, figs. 2.9, 2.10, 2.13) has three different regime diagrams, two based on subjective criteria with different regime names (one archaic, the other state-of-the-art), and another based on objective breakup length data with completely different regime names. The subjective and objective regimes have been unified in the past (Reitz, 1978, p. 165, fig. 1.1), though this is not always done. In this work, a fully unified regime diagram will be proposed such that the objective and subjective classifications are consistent.

Reitz (1978, pp. 4-9) has a detailed discussion of earlier research into the boundaries of the breakup regimes, which for the most part remains current — Reitz's work continues to be cited by more recent reviews (Birouk and Lekic, 2009; Chigier and Reitz, 1996; Lefebvre and McDonell, 2017; and Lin and Reitz, 1998). Several criteria have been proposed, to be discussed in the next subsection. These criteria have not been treated as unimpeachable, but at least accurate enough to use for the planning of experiments in a particular regime.

A summary of past regime studies is in table 1. The first regime diagram was due to von Ohnesorge (2019) in 1936 and is reproduced in figure 2. The regime diagram can be used to determine the regime by computing the nozzle Reynolds number $\mathrm{Re}_{\ell 0}$ and also what today is called the Ohnesorge number $\mathrm{Oh}_{\ell 0} \equiv \mu_\ell/(\rho_\ell \sigma d_0)$, which von Ohnesorge called Z. By computing $\mathrm{Re}_{\ell 0}$ and $\mathrm{Oh}_{\ell 0}$, an engineer can determine the regime by the location of the point in figure 2 (with some caveats; the nozzle and liquid-gas density ratio need to be similar to von Ohnesorge's). While some modifications to von Ohnesorge's diagram have been made since 1936, nearly the same regime diagram is used today as can be seen in the recent book of Lefebvre and McDonell (2017, figs. 2.9, 2.10).

The Ohnesorge number is independent of the velocity, which means that in these coordinates, increasing the velocity only changes the Reynolds number. Alternative coordinates (including the one I propose) lack this property, which I believe does not outweigh the disadvantages of using the Ohnesorge number. Regime boundaries are typically given in terms of constant gas or liquid Weber numbers, so it would make more sense to create a plot in terms of the Weber and Reynolds numbers, as I did in figure 3. A similar plot has been made by Faeth (1991, fig. 2) previously. The reader may find this plot easier to understand.

Some studies in table 1 focused on a single regime boundary rather than a complete diagram (Grant and Middleman, 1966; Kusui, 1969; Miesse, 1955; and Sterling and Sleicher, 1975). The majority of previous studies classified regimes based on subjective evaluation of photographs (9 out of 13 considered). The majority of previous studies also only considered a relatively small amount of data, e.g., 8 out of 13 studies considered had less than 100 data points in total, making their regime diagrams based on rather sparse data. For that reason, in the data compilation used to construct the new regime diagram in this work, as much objective data as possible was collected. As shown in table 1, this work uses roughly an order of magnitude more data than any previous study. This gives the regime diagram in this work much more resolution and also range than previous regime diagrams. The Reynolds number ranges from 5.9 to 7.3×10^5 in this work, and the Weber number ranges from 2.0 to 4.1×10^5.

Rough pipe data from Kusui (1969) was used to determine the variation of one regime boundary with the turbulence intensity. The turbulence intensity could be credibly estimated in only a few additional previous studies. (The estimation of the turbulence intensity will be discussed later in § 4.1.)

3. ISSUES WITH PREVIOUS REGIME DIAGRAMS

Figures 2 and 3 have many issues, the most significant of which will be detailed in this section.

3.1 Little data justifying most of the boundaries

The most egregious problem with the most commonly used boundaries as represented in figure 3 is how little data they are based on. 3 out of 4 of the regime boundaries in figure 3 come from Ranz (1956, p. 61):

$$\text{dripping if} \quad \mathrm{We}_{\ell 0} < 8 \tag{1}$$

$$\text{Rayleigh if} \quad \mathrm{We}_{\mathrm{g}0} < 0.4 \quad (\text{and } \mathrm{We}_{\ell 0} > 8) \tag{2}$$

$$\text{first wind-induced if} \quad \mathrm{We}_{\mathrm{g}0} < 13 \quad (\text{and } \mathrm{We}_{\mathrm{g}0} > 0.4). \tag{3}$$

These boundaries are purely theoretical, based on no data at all. The derivations are missing from Ranz's report, but they appear to be based on simple scaling arguments based on supposed

TABLE 1: Previous regime studies.

	Photos	$\langle x_\mathrm{b} \rangle$	**Total**
Haenlein (1932)	24	0	24
von Ohnesorge (2019)	63	0	63
Littaye (1942, fig. 47)	52	0	52
Miesse (1955, fig. 8)	66	0	66
Ranz (1956, pp. 61–62)	0	0	0
Grant and Middleman (1966)	26	127	132
Kusui (1969)	0	158	158
Sterling and Sleicher (1975)	0	106	106
Torda (1973, fig. 14)	12	0	12
Reitz (1978, pp. 133–137)	67	0	67
Wu et al. (1995, fig. 7)	110	0	110
Tang and Masutani (2003)	75	0	75
Schillaci et al. (2019)	11	0	11
This work	119	1094	1187

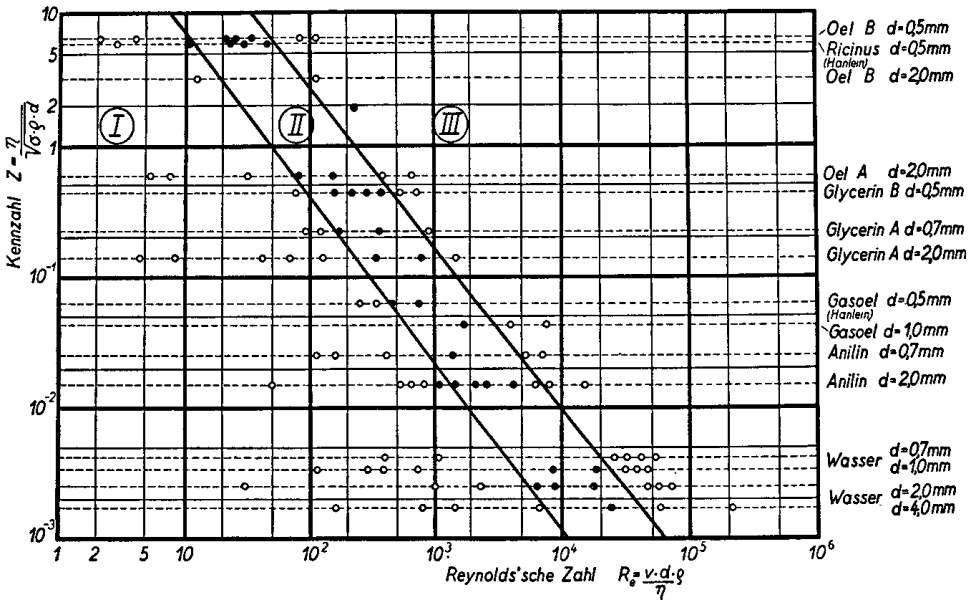

FIG. 2: The original regime diagram of von Ohnesorge (2019).

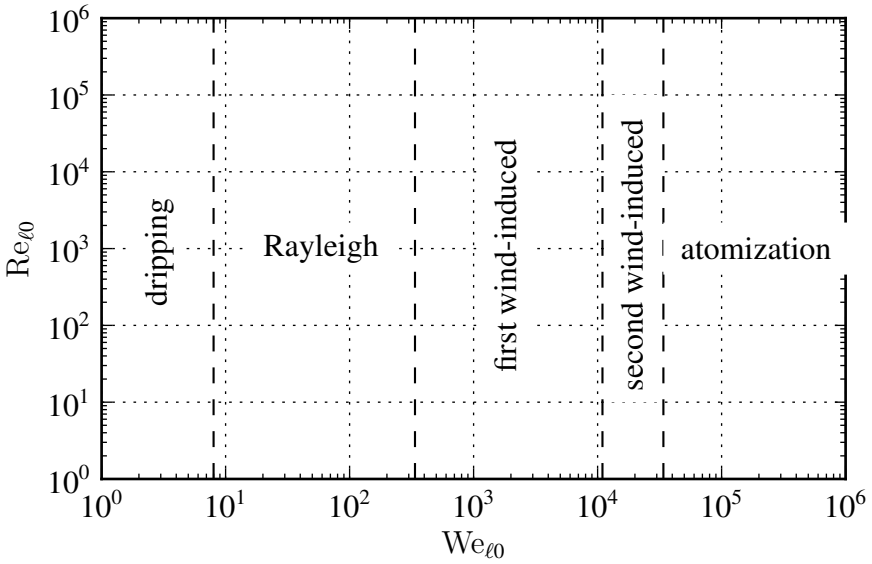

FIG. 3: The most popular regime diagram in liquid Weber number and liquid Reynolds number coordinates for liquid water injected into atmospheric air at 25 °C. These coordinates are preferred over those used in figure 2 because most engineers have better intuitions for the Weber number than the Ohnesorge number, and the regime diagram is simplified in these coordinates. Note that in this regime diagram, 3 of 4 of the regime boundaries will move if the liquid-gas density ratio is changed.

physics. There is no comparison against experimental data in Ranz's report (as written in table 1). As it turns out, some of these assumptions end up being poor, for example, the suggestion that the transition to what Ranz calls the atomization regime, which was later called the second wind-induced regime (Chigier and Reitz, 1996, p. 114), is caused by the influence of ambient gas is found to be false in § 3.3 of this work. While these boundaries could be worse, they are not particularly accurate when compared against the new regime diagram developed in this work.

3.2 The most common atomization regime boundary was miscalculated

The most popular atomization regime boundary criteria is $\mathrm{We}_{\mathrm{g0,crit}} = 40.3$, and this boundary is used in figure 3. This boundary was developed from a different equation from Miesse (1955, p. 1698R) that itself used a functional form proposed by Littaye (1944). Miesse conducted photographic experiments and proposed the regime boundary equation

$$\mathrm{Oh}_{\mathrm{l}0} = C_{\mathrm{Miesse}} \mathrm{Re}_{\ell 0}^{-\alpha_{\mathrm{Miesse}}}, \tag{4}$$

where $C_{\mathrm{Miesse}} = 100$ and $\alpha_{\mathrm{Miesse}} = 0.92$. Reitz (1978, p. 8) modifies this equation to the form $\mathrm{We}_{\mathrm{g0,crit}} = 40.3$*. If α_{Miesse} is set equal to 1 then

$$\mathrm{Oh}_{\ell 0} \mathrm{Re}_{\ell 0} = C_{\mathrm{Miesse}}. \tag{5}$$

*Also see the summary by Chigier and Reitz (1996, p. 113).

TABLE 2: Regime name conversions.

New regime name	Old regime name
dripping	dripping
laminar Rayleigh	Rayleigh
laminar non-Rayleigh	first wind-induced
turbulent Rayleigh	—
turbulent surface breakup	second wind-induced
(turbulent) atomization	atomization

Note that $\mathrm{Oh}_{\ell 0}\mathrm{Re}_{\ell 0} \equiv \sqrt{\mathrm{We}_{\ell 0}}$. Consequently, the critical liquid Weber number is

$$\mathrm{We}_{\ell 0,\mathrm{crit}} = C^2_{\mathrm{Miesse}}. \tag{6}$$

Reitz proposes that this is actually a critical gas Weber number, so

$$\mathrm{We}_{\mathrm{g}0,\mathrm{crit}} = \frac{\rho_\mathrm{g}}{\rho_\ell}\mathrm{We}_{\ell 0,\mathrm{crit}} = \frac{\rho_\mathrm{g}}{\rho_\ell}C^2_{\mathrm{Miesse}}. \tag{7}$$

Using the previous result, $\mathrm{We}_{\mathrm{g}0,\mathrm{crit}} = 40.3$ implies a density ratio of $\rho_\ell/\rho_\mathrm{g} \approx 250$, which is inconsistent with Miesse's experiment. Miesse used water in ambient air and liquid nitrogen in air (Miesse, 1955, p. 1694L). Based on the numbers included in Miesse's paper, the density ratio for water in air was $\rho_\ell/\rho_\mathrm{g} = 742$ and the the density ratio for liquid nitrogen in air was $\rho_\ell/\rho_\mathrm{g} = 671$. Using the density ratio for water in air returns $\mathrm{We}_{\mathrm{g}0,\mathrm{crit}} = 12$. This is more consistent with Ranz (1956, p. 61), who proposes that $\mathrm{We}_{\mathrm{g}0,\mathrm{crit}} = 13$ as the onset of atomization, although as stated previously, that limit was later associated with the onset of the second wind-induced regime.

The existing regime boundaries are either based on no data at all, or based on a miscalculation. This situation is unacceptable, and the heavily data-driven regime diagram developed here is intended to remedy this.

3.3 Regime names

In this work I use the phase "turbulent surface breakup" instead of "second wind-induced", and "laminar non-Rayleigh" instead of "first wind-induced". The "wind-induced" regime names do not accurately describe the physical mechanisms involved. Many past researchers believe that breakup in these regimes is caused mainly by ambient gas effects (Dumouchel, 2008; Lin and Reitz, 1998; and Reitz, 1978), but my own analyses cast doubt on these assertions. To be more specific, in the "second wind-induced" (i.e., turbulent surface breakup) regime I find no influence of the ambient gas at all Trettel (2020a,b), which makes the "wind-induced" name seem inappropriate. Sallam (2002, p. 94) agrees with this assessment. The so-called "first wind-induced" regime appears to at least sometimes have a dependence on the ambient gas, though other factors like turbulence transition and velocity profile relaxation (both possibly influenced by the ambient environment) appear to be factors as well. However, without the second wind-induced regime, a regime called the first wind-induced regime seems misplaced, so I've chosen the name "laminar non-Rayleigh" instead. This name is tentative as I believe there are multiple regimes contained within the laminar non-Rayleigh regime; see § 4.6 for details.

Table 2 shows the conversion between the regime names proposed in this work and the conventional regime names.

3.4 Turbulence transition

It is important to consider how hydrodynamic regimes (i.e., turbulent vs. laminar) affect breakup regimes. One would expect turbulence transition to cause a change in the breakup regime. I first realized this after seeing that there was no turbulence transition in the original Ohnesorge diagram, figure 2. This oversight becomes even more egregious in figure 3, which is in coordinates I and most engineers are more comfortable with.

Based on the data I've compiled, which is limited to jets produced by long pipes, the transition from the laminar non-Rayleigh regime to the turbulent surface breakup regime appears to be caused by a turbulence transition in the nozzle. This is most easily seen in the data of Grant and Middleman (1966, fig. 11, p. 675R), who classified the nozzle outlet flow as laminar or turbulent.

Unfortunately, the most popular regime diagram as expressed through figure 3 does not distinguish between jets which are turbulent or laminar at the nozzle outlet, despite the clear effects this has on the jet breakup.

In this work the new regime diagram has a critical Reynolds number for the start of transition $\mathrm{Re}_{\ell 0,\mathrm{crit}}$ and also a second critical Reynolds number for the establishment of fully turbulent flow $\mathrm{Re}_{\ell 0,\mathrm{turb}}$. The numbers used in figure 4 are 2300 and 4000, respectively. These will vary from system to system in potentially difficult to predict ways, even for fully developed pipe flows (Mullin, 2011). Laminar flows at the nozzle outlet have been observed at Reynolds numbers two orders of magnitude higher that those seen in pipe flows. Typically at higher Reynolds numbers the jet transitions to turbulence after a short distance. For simplicity, it can be convenient to refer to a single transitional Reynolds number, $\mathrm{Re}_{\ell 0,\mathrm{crit}}$. Because the transition Reynolds number can vary greatly, breakup regime diagrams must consider the transitional Reynolds number as a variable. Reviewing the literature on the critical Reynolds number of nozzles and pipes is prudent.

As mentioned, laminar nozzle flows have been observed at Reynolds numbers as high as $\mathrm{Re}_{\ell 0} = 2 \times 10^5$ (Hoyt and Taylor, 1977, fig. 2). With that being said, the transition Reynolds number for a nozzle flow can be comparable to that of a pipe flow. For example, appreciable turbulence intensities were measured by Lebedev (2019) for a nozzle presumably like a diesel injector at Reynolds numbers of about 1×10^3. Presumably the nozzle was roughened, as Tonkonogiy et al. (1990) shows that the critical Reynolds number of a rough pipe can decrease below that of a smooth pipe:

$$\mathrm{Re}_{\ell 0,\mathrm{crit}} = \min\left[38\left(\frac{\epsilon}{d_0}\right)^{-0.8}, \sim 2000\right], \tag{8}$$

where ϵ is the height of the roughness elements used in the experiments of Tonkonogiy et al..

The critical Reynolds number is also a function of the nozzle length. van de Sande and Smith (1976, pp. 220R–221L, eqn. 10) conducted experiments and constructed the following empirical regression for the critical Reynolds number as a function of the dimensionless nozzle length L_0/d_0, valid for $1 \leq L_0/d_0 \leq 100$:

$$\mathrm{Re}_{\ell 0,\mathrm{crit}} = 1.2 \times 10^4 \left(\frac{L_0}{d_0}\right)^{-0.3}. \tag{9}$$

The contraction ratio of these experiments was very large ($d_{\mathrm{in}}/d_{\mathrm{out}} > 150$), so presumably the flow was stabilized due to relaminarization. With smaller contraction ratios, likely the critical Reynolds number is lower than implied by equation 9. Due to the power law form, the critical Reynolds number implied by equation 9 will not saturate at large L_0/d_0 as one might expect

when the flow becomes fully developed. Consequently, to predict the critical Reynolds number if the nozzle length is longer than $100d_0$ it is recommended to use $L_0/d_0 = 100$ instead of the actual nozzle length.

As a check on this equation, a regime plot of Wu et al. (1995, fig. 7) can be used to develop a very approximate critical Reynolds number equation ($\mathrm{Re}_{\ell 0,\mathrm{crit}} \approx 4.7 \times 10^4 (L_0/d_0)^{-0.22}$) which is similar to equation 9. Equation 9 is recommended over the equation this latter equation due to the likely better accuracy. One difference is worth noting: Wu et al. do not observe turbulence at the nozzle outlet for $L_0/d_0 < 6$ but van de Sande and Smith do. The reason for this difference is unknown, and highlights the difficulty of predicting turbulence transition.

Interestingly, apparently all data in the classic regime study of von Ohnesorge (2019) was laminar at the nozzle outlet. This actually has major consequences for the regime diagram, which are discussed in § 4.6. It is possible that previous regime diagrams did not distinguish between laminar and turbulent flows because all flows observed were laminar at the nozzle outlet. This is not to say that initially laminar jets will never breakup up due to turbulence. These jets tend to transition to turbulence externally; they are merely initially laminar.

Some of the jet breakup data compiled in this work apparently had unusually high critical Reynolds numbers for pipe flows, i.e., for Eisenklam and Hooper (1958) and Sterling and Sleicher (1975), $\mathrm{Re}_{\ell 0,\mathrm{crit}} = \mathcal{O}(10^4)$. These studies were neglected for that reason, as they are inconsistent with other studies. It is not unheard of to have critical Reynolds numbers higher than those typical for pipe flows. Pfenniger (1961) observed $\mathrm{Re}_{\ell 0,\mathrm{crit}} = \mathcal{O}(10^5)$ by taking care to eliminate flow disturbances. Mullin (2011) notes that a high critical Reynolds number is a good measure of the quality of an experimental facility.

3.5 Turbulence intensity effects

Reitz (1978, p. 9) notes that the conventional regime boundaries do not correctly predict the regime in water jet cutting, where the jets appear to be considerably more stable and consequently in "earlier" regimes than the standard criteria would suggest. Reitz (1978, p. 9) attributes these violations to "nozzle geometry effects" The turbulence intensity can explain this discrepancy, as the turbulence intensity would be lower in cutting water jets than the fuel sprays typically studied. The more recent study of Tafreshi and Pourdeyhimi (2003) shows another violation of the earlier regime boundaries likely due to turbulence intensity effects.

Existing regime diagrams suffer from poor reproducibility due to neglecting several turbulence related variables like the critical Reynolds number and turbulence intensity. General regime criteria need to take into account fundamental physics, and not be mere regressions which apply only to particular cases. Consequently, a goal of this work is to include turbulence intensity as a variable wherever possible.

3.6 Lack of intuition with the Ohnesorge number

While the Ohnesorge number has the useful property of being independent of the jet bulk velocity (as discussed in § 2), the vast majority of engineers have little to no intuition for the quantity. A regime diagram based on more familiar dimensionless quantities would be preferred. Now there are diagonal lines for a particular nozzle and fluid in the regime diagram as the velocity increases. See figure 5. These are lines of constant Ohnesorge number. While having diagonal rather than horizontal lines is less simple, I believe the gains in intuition from avoiding the Ohnesorge number are a vast improvement.

TABLE 3: Subjective characteristics of each regime.

Regime name	Appearance
dripping	slow formation of droplets at the nozzle outlet
laminar Rayleigh	symmetric breakup into large droplets
laminar non-Rayleigh	varies from Rayleigh-like to abrupt breakup
turbulent Rayleigh	similar to laminar Rayleigh, but turbulent
turbulent surface breakup	small surface disturbances causing breakup
(turbulent) atomization	larger spray angle than turbulent surface breakup

TABLE 4: Objective characteristics of each regime.

Regime name	$\langle x_\mathrm{b} \rangle / d_0$	D_{32}
dripping	$\gtrsim \left(\frac{\mathrm{Fr}_0}{\mathrm{We}_{\ell 0}} \right)^{1/3}$	$\mathcal{O}(d_0)$
laminar Rayleigh	$\propto \mathrm{We}_{\ell 0}^{1/2} + 3 \frac{\mathrm{We}_{\ell 0}}{\mathrm{Re}_{\ell 0}}$	$\mathcal{O}(d_0)$
laminar non-Rayleigh	decreasing with $\overline{U}_0$	varies
turbulent Rayleigh	$\propto \mathrm{We}_{\ell 0}^{1/2} + 3 \frac{\mathrm{We}_{\ell 0}}{\mathrm{Re}_{\ell 0}}$	$\mathcal{O}(d_0)$
turbulent surface breakup	$\gtrsim \mathrm{We}_{\ell 0}^{1/3}$	$< d_0$
(turbulent) atomization	$\gtrsim \left(\frac{\rho_\ell}{\rho_\mathrm{g}} \right)^{C_\rho}$	$\ll d_0$

This is not to say that the Ohnesorge number is useless, just that it should be regarded as secondary to the Reynolds and Weber numbers in the regime diagram. If $\mathrm{Re}_{\ell 0,\mathrm{crit}}$, $\overline{\mathrm{Tu}_0}$, and $\rho_\ell / \rho_\mathrm{g}$ are constant, then the regime progression (to be discussed) is determined by the Ohnesorge number. This situation is approximately satisfied in many situations

3.7 Subjective vs. objective classification

Regimes are often defined in qualitative ways based on photographs or vague descriptions (e.g., see table 3). These regimes are somewhat subjective. This is particularly problematic for the atomization regime, as it's superficially similar to the turbulent surface breakup regime, just more vigorous in some sense. Consequently, I define objective criteria to determine the regimes based on breakup length in table 4 (discussed earlier as well). In this work I also unify the visual and breakup length regimes so that each "breakup length" regime has an associated appearance, though it may not be always possible to go the other direction, from the appearance to the regime, due to ambiguities in the appearance.

The next problem is partly caused by the superficial nature of subjective regime determination.

3.8 A missing regime and the varying regime progression

When a liquid jet is in the Rayleigh regime and the velocity is increased (all else equal), convention and the Ohnesorge diagram stipulate that the jet will eventually transition to the first wind-induced regime. This is not necessarily true. The "regime progression", that is, how the

regimes change as the jet velocity increases, is not universal.

While the majority of jets previously studied will transition to the first wind-induced regime after "the" Rayleigh regime, some researchers have identified a *turbulent Rayleigh* regime that is different from the conventional *laminar Rayleigh* regime (Mansour and Chigier, 1994; Phinney, 1973, 1975; Sallam et al., 2002). This regime is missing from the traditional Ohnesorge diagram. The turbulent Rayleigh regime is sometimes superficially visually similar to the first wind-induced. Compare figure 10, a jet early in the first wind-induced regime, against figure 13. The two appear to be visually similar to laminar Rayleigh (see figure 9 for an example), although less regular.

However, the breakup length decreases as velocity increases in the first wind-induced regime, but increases as velocity increases in the turbulent Rayleigh regime. Typically, the first wind-induced regime is defined as having a decreasing breakup length, e.g., by Reitz (1978, fig. 1.1) and Dumouchel (2008, fig. 1). Many studies have examined the first decrease in the breakup length curve, motivated by the first wind-induced regime; see Dumouchel (2008) and Leroux et al. (1996) for a review of these studies. However, the breakup length can also decrease due to turbulence transition in the nozzle ($\mathrm{Re}_{\ell 0} > \mathrm{Re}_{\ell 0,\mathrm{crit}}$). And once turbulent flow is established, the breakup length then will increase proportional to $\mathrm{We}_{\ell 0}^{1/2} + 3\mathrm{We}_{\ell 0}/\mathrm{Re}_{\ell 0}$, just like in the laminar Rayleigh regime, albeit with a lower constant of proportionality (Mansour and Chigier, 1994, fig. 5). As such, I define the first wind-induced regime as laminar at the nozzle outlet, in contrast to previous researchers like Reitz (1978, p. 24). The data compilation detailed in this work shows that the first wind-induced regime only appears when the flow is laminar at the nozzle outlet.

Mistaking the first wind-induced and turbulent Rayleigh regimes is not uncommon, e.g., in his work on the regime diagram, Reitz (1978, pp. 24–25) suggests that the experiments of Phinney (1973) are in the first wind-induced regime, but these experiments are actually largely in the turbulent Rayleigh regime.

The regime progression is not universal. Examine the three diagonal lines in figure 5. The middle line is the "conventional" case, that is, where the jet transitions from the (laminar) Rayleigh regime to the laminar non-Rayleigh regime, then to the turbulent surface breakup regime, and then to the atomization regime. The trends in the breakup length for this case are show in figure 6. The "conventional" case is only one of several possibilities and may not actually be typical. A larger pipe nozzle with a low viscosity liquid follows the path shown by the upper diagonal line in figure 5. This case never enters the laminar non-Rayleigh regime as seen in figure 7. A more typical case is that seen for a higher viscosity liquid like diesel fuel with a smaller nozzle (same diameter as the Spray A nozzle), corresponding to the lower diagonal line. This case, which is likely common in practice, never enters the turbulent surface breakup regime, as seen in figure 8.

Another way in which the regime progression is not universal comes through the influence of the critical Reynolds number. This has been recognized by previous researchers. Eisenklam and Hooper (1958, fig. 14) noticed that if they add a turbulence trip inside of their nozzle, they can avoid what they called "bursting breakup", which is a particularly violent form of breakup in the laminar non-Rayleigh regime (see figure 11 for an example). Similarly, Hoyt and Taylor (1985) suggest moving turbulence transition inside of the nozzle, or in other words, decreasing the nozzle critical Reynolds number, to avoid very vigorous breakup (identical to "bursting breakup") apparently caused by external turbulence transition.

3.9 Breakup onset location in atomization

The atomization regime is sometimes defined as when $\langle x_\mathrm{i} \rangle$ is very small, indistinguishable from zero (Reitz and Bracco, 1986, p. 235). This definition is unsatisfactory as $\langle x_\mathrm{i} \rangle$ can also be small in the turbulent surface breakup regime. The $\langle x_\mathrm{i} \rangle$ theory in Trettel (2020a) applies to both the turbulent surface breakup and atomization regimes. Consequently, I define the atomization regime based on more obvious objective criteria: the breakup length curve. I define the turbulent surface breakup regime as having an increasing power law behavior in $\langle x_\mathrm{b} \rangle$ as a function of $\mathrm{We}_{\ell 0}$ ($\langle x_\mathrm{b} \rangle / d_0 \precsim \mathrm{We}_{\ell 0}^{1/3}$), and the atomization regime is defined as a plateau as $\mathrm{We}_{\ell 0}$ increases, all else constant and neglecting cavitation and Mach number effects (to be discussed later).

3.10 Problems with other regime diagrams

Wu and Faeth (1993) suggests that $\rho_\ell / \rho_\mathrm{g} < 500$ is a reasonable criteria for the onset of aerodynamic effects, in this work called the atomization regime. Magnotti (2017) later suggested that $\rho_\ell / \rho_\mathrm{g} < 300$ is a more accurate criteria for the onset of aerodynamic effects. Purely density ratio based criteria are not accurate, as increasing the velocity alone can change the regime from turbulent surface breakup to atomization (Kusui, 1969 and Sallam et al., 2002). The differences in the boundaries observed by Wu and Faeth and Magnotti likely could be attributed to differences in the Weber numbers and turbulence intensities.

4. PROPOSED REGIME DIAGRAM AND INFORMATION ON EACH REGIME

The proposed regime diagram is shown in figure 4. A sample of data for high liquid-gas density ratios and smooth pipe nozzles is shown in figure 5 to give a sense for how well these boundaries fit the data. In contrast with figure 4, which is for constant turbulence intensity, in figure 5 the turbulence intensity is a function of the Reynolds number, which is why some of the regime boundaries are not straight lines as they are in figure 4.

Individual regime boundaries were developed in various ways, using all data available for that boundary (i.e., not only high density ratio data as in figure 4), as described in the corresponding section for that boundary.

A warning: The proposed regime diagram is not meant to be used as presented to determine the regime. It is a *schematic* used to organize knowledge about the regimes. Regime determination is best done with the empirical equations developed in this work for each regime boundary. This is because the regime boundaries will move depending on the configuration. Figure 4 is really only appropriate for pipe nozzles at high liquid-gas density ratios.

Historically, the Ohnesorge diagram has sometimes been applied robotically to determine the regime, obtaining results which seem at odds to the visual descriptions of the regimes. Unfortunately not all engineers have noticed the discrepancies. I suggest to all readers of this work to not hesitate to challenge the regime diagram if it contradicts your understanding.

4.1 Data compilation

The proposed regime diagram is based on a compilation of data described in detail in Trettel (2020b) and will only be briefly described here. This data compilation uses "pipe jet" data, where the nozzle is simply a long pipe. Pipe jets were chosen for their ubiquity in the literature, their high reproducibility (due to fully developed flows being a universal state), and because

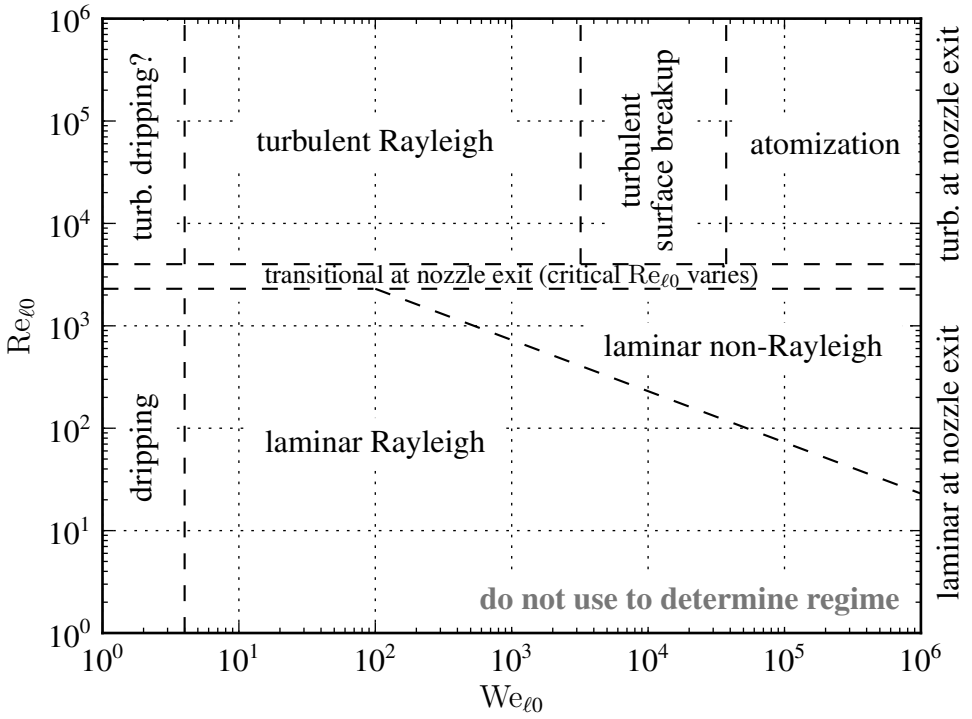

FIG. 4: Schematic regime diagram at low ambient densities *for illustration purposes only*. Do not use this plot to determine the regime. Regime boundaries are very approximate and apply only for a special case. More precise boundaries are given in the text. The critical Reynolds number (and correspondingly, the Reynolds number where fully turbulent flow is established) will typically be an order of magnitude or more higher than in this plot, which is based on long pipe nozzles (fully developed pipe flow) that have atypically low critical Reynolds numbers. Constant high density ratio ($\rho_\ell/\rho_g = 1000/1.2$) corresponding approximately to water-air at standard temperature and pressure. Turbulence intensity is 5%. Turbulent regime boundaries should vary with Reynolds number in a smooth pipe due to variation of turbulence intensity with the Reynolds number — see figure 5.

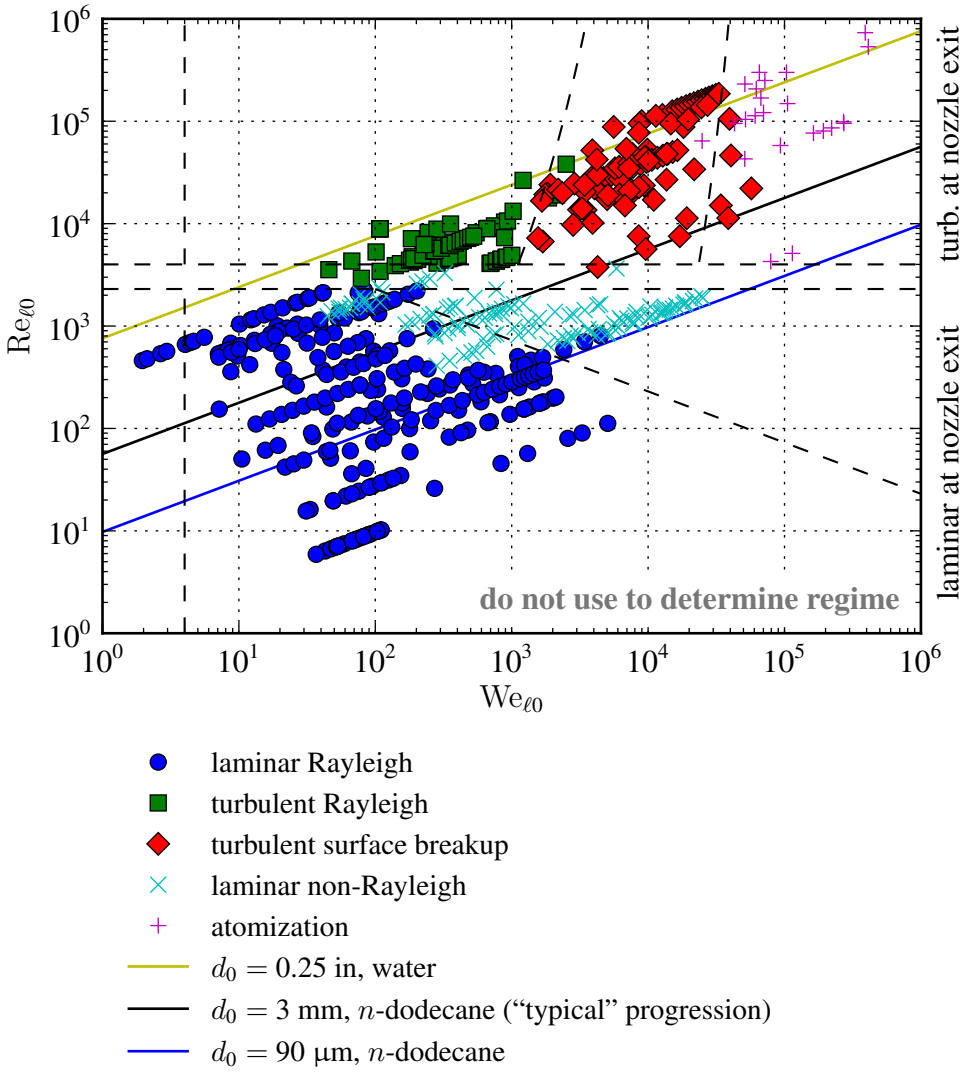

FIG. 5: Regime diagram for smooth pipe nozzles with data and example lines showing the regime progression for two different nozzles and fluids. Transitional regimes removed for clarity. Data from Eisenklam and Hooper (1958) and Sterling and Sleicher (1975) removed due to abnormally high transitional Reynolds numbers. 556 data points. In contrast with figure 4, the turbulence intensity is now a function of the Reynolds number (as is the case for a smooth pipe flow), and consequently the turbulent regime boundaries vary with Reynolds number. High density ratio data only ($\rho_\ell/\rho_\mathrm{g} > 500$). Atomization regime boundary for $\rho_\ell/\rho_\mathrm{g} = 1000/1.2$.

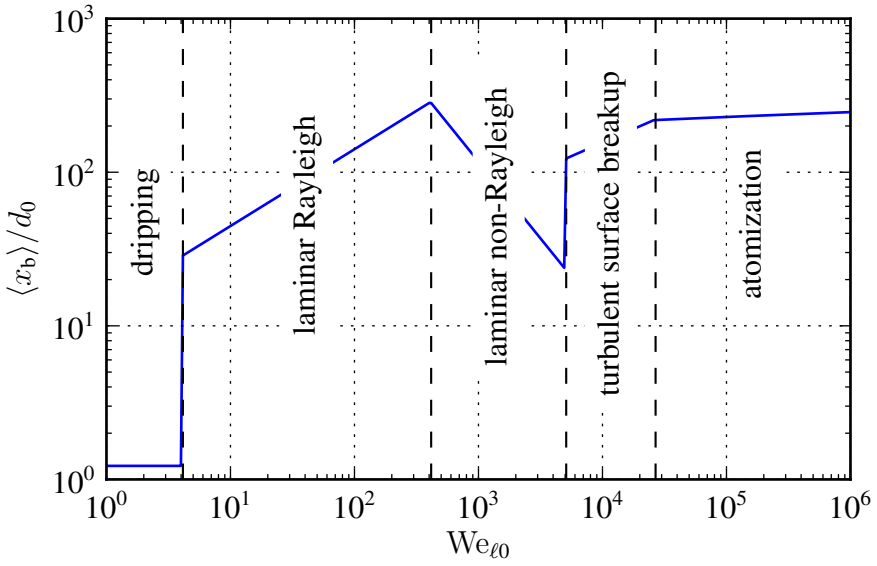

FIG. 6: *Schematic* "stability curve" for the "conventional" pipe nozzle case in figure 5. Regression equations for the breakup length $\langle x_\mathrm{b}\rangle$ from the text are used in each marked regime above. Breakup lengths for the "laminar non-Rayleigh regime" are approximate, and the real stability curve will be smoother. Note that like in figure 5, the turbulence intensity $\overline{\mathrm{Tu}_0}$ and Reynolds number $\mathrm{Re}_{\ell 0}$ are changing as the Weber number $\mathrm{We}_{\ell 0}$ changes.

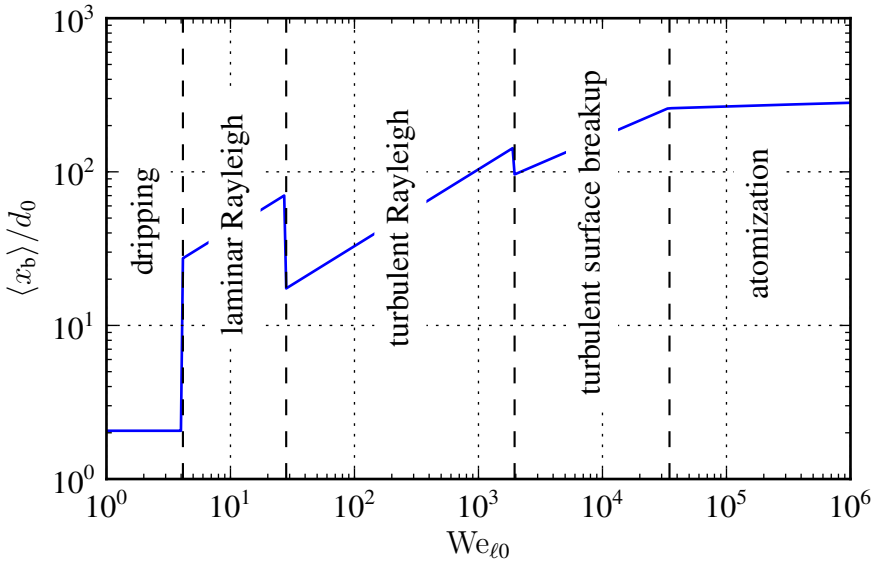

FIG. 7: *Schematic* "stability curve" for the pipe nozzle $d_0 = 0.25$ in, water case in figure 5. See figure 6 for details.

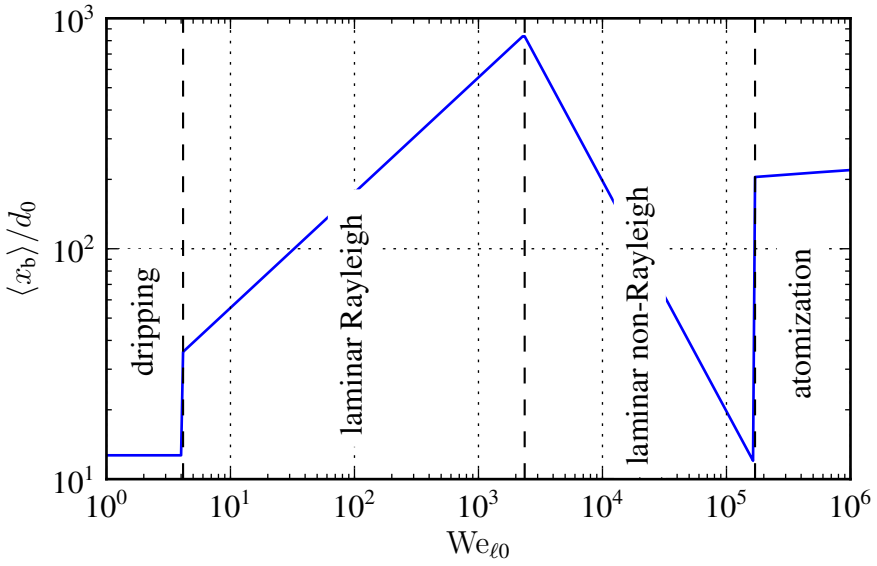

FIG. 8: *Schematic* "stability curve" for the pipe nozzle $d_0 = 90$ µm, n-dodecane (similar to Spray A but with a lower $\mathrm{Re}_{\ell 0,\mathrm{crit}}$) case in figure 5. See figure 6 for details.

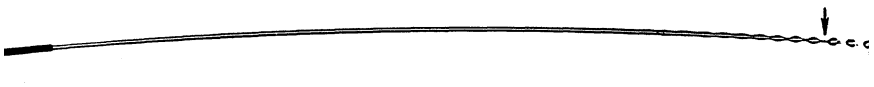

FIG. 9: Photograph of a water jet in the laminar Rayleigh regime from Grant (1965, fig. 5-3a). Note the breakup is caused by disturbances symmetric to the jet axis. The arrow indicates the location of breakup. Flow is from left to right.

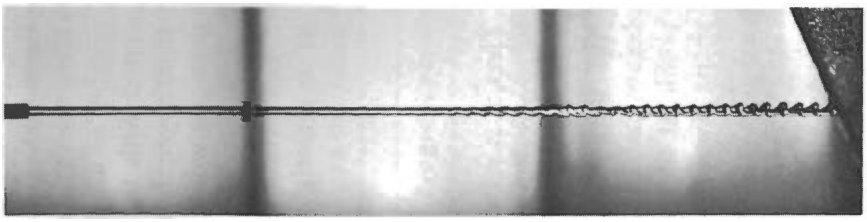

FIG. 10: Photograph of a water jet early in the laminar non-Rayleigh regime from Rupe (1962, fig. 4c). Flow is from left to right.

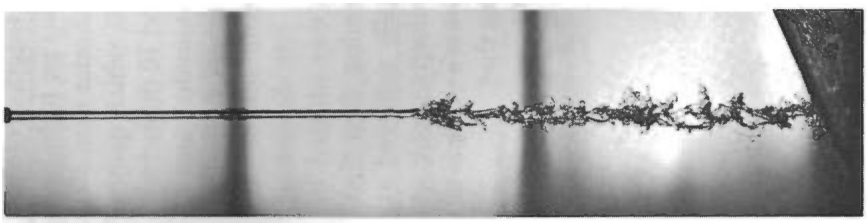

FIG. 11: Photograph of a water jet late in the laminar non-Rayleigh regime from Rupe (1962, fig. 4d) which is atomization-like. Note that the breakup is much more vigorous than that seen in figure 10. Flow is from left to right.

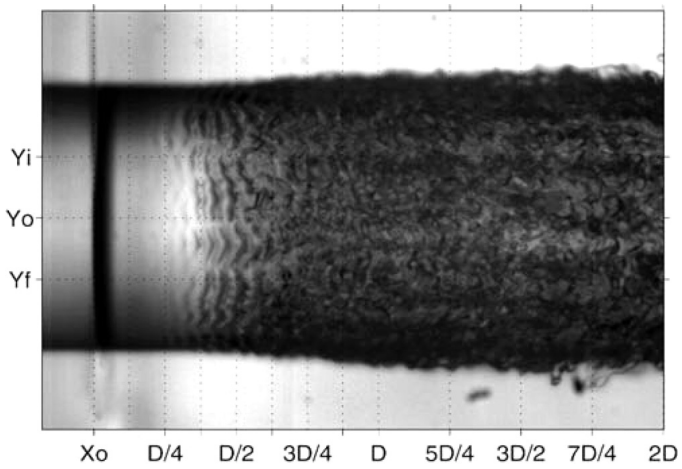

FIG. 12: Photograph of a water jet in the laminar non-Rayleigh regime from Portillo et al. (2011, fig. 2). Here the breakup is more vigorous than that seen in figure 10, but less vigorous than figure 11. This jet is in a regime similar to the turbulent surface breakup regime. Unlike the other photographs, which use pipe nozzles, this for a nozzle with an aspect ratio $L_0/d_0 = 1$. Flow is from left to right.

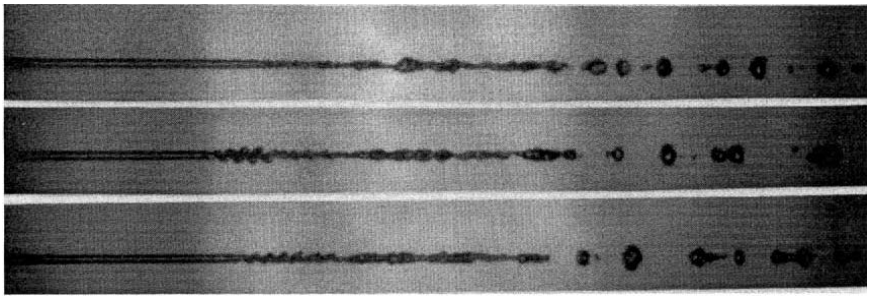

FIG. 13: Photograph of a water jet in the turbulent Rayleigh regime from Sallam et al. (2002, fig. 2). Flow is from left to right.

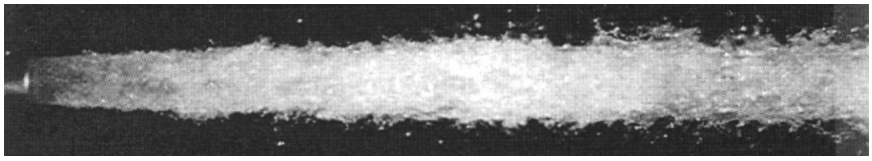

FIG. 14: Near-nozzle photograph of a water jet in the turbulent surface breakup regime from Wu (1992, fig. 4-2b). Flow is from left to right.

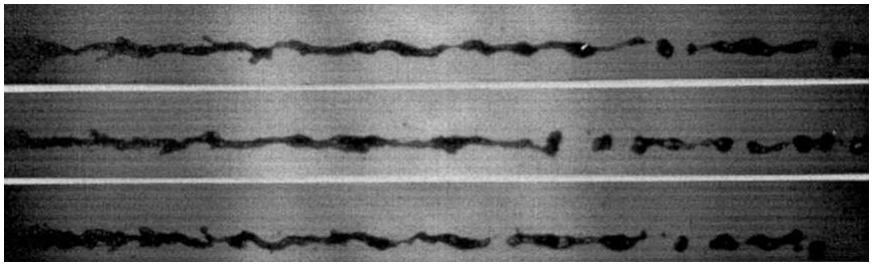

FIG. 15: Downstream (near breakup length) photograph of a water jet in the turbulent surface breakup regime from Sallam et al. (2002, fig. 3). Flow is from left to right.

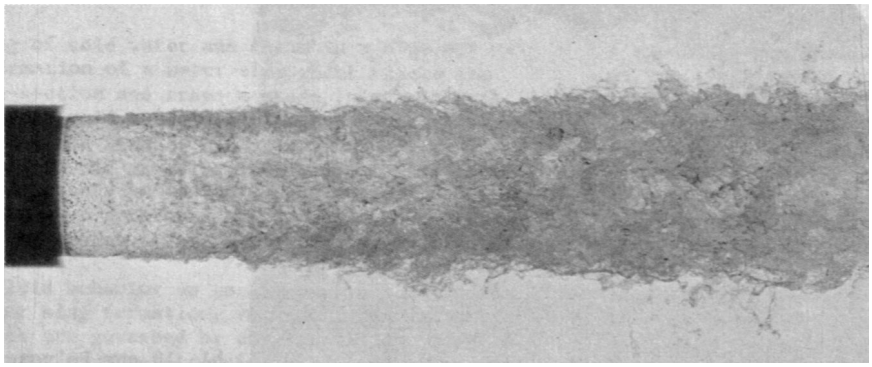

FIG. 16: Near-nozzle photograph of a water jet believed to be in the atomization regime from Hoyt and Taylor (1980, fig. 1a). Note the similarity to figure 14; determining if a jet is in the turbulent surface breakup or atomization regime based on visual characteristics alone is challenging. Flow is from left to right.

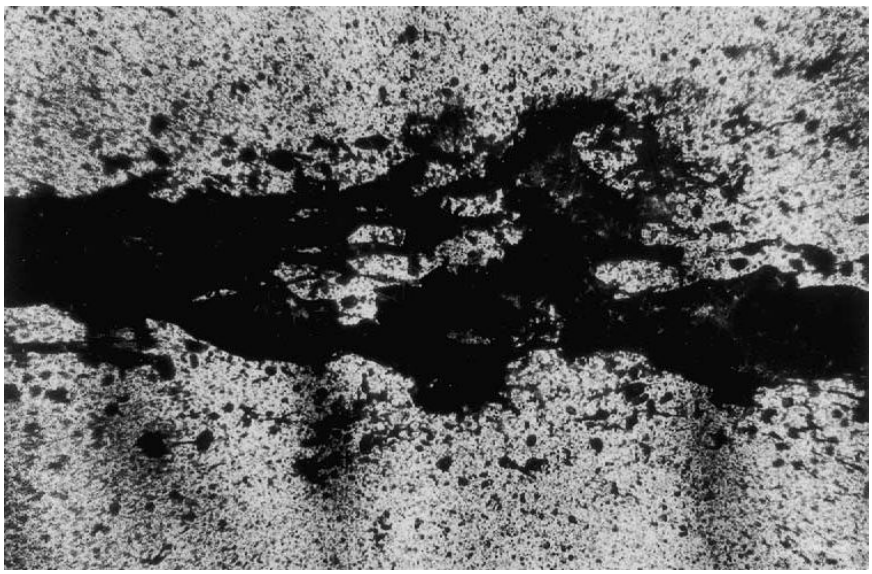

FIG. 17: Downstream photograph of a water jet in the atomization regime from Sallam et al. (2002, fig. 6). Flow is from left to right.

turbulence intensity can be determined for them given the friction factor. Data from over 20 different studies was compiled.

Turbulence intensity (defined in this work as $\overline{\mathrm{Tu}_0} \equiv (2\overline{k}_0/3)^{1/2}/\overline{U}_0$) was estimated using a regression between the friction factor and $\overline{\mathrm{Tu}_0}$ for fully developed pipe flows: $\overline{\mathrm{Tu}_0} = 0.366 f^{0.459}$ (9 smooth and 8 rough points, $R^2 = 0.975$). Generally turbulence intensity is roughly constant for smooth pipe flows. Rough pipe data from Kusui (1969) was used to vary the turbulence intensity from 0.049 to 0.127.

4.2 Regimes and their physical mechanisms

More detailed descriptions and analysis of each regime follows, going from left to right in figure 4, starting with the regimes with flows that are laminar at the nozzle outlet and following with the regimes with flows that are turbulent at the nozzle outlet.

Some sections will contain regressions for the breakup length. Some of these regressions come from previous works, and others are developed in this work. The regressions developed in this work will be presented without comment on how they were obtained. The reader is referred to other works using the same data compilation to understand the theory and choice of functional forms Trettel (2020a,b).

4.3 Dripping regime and transition to jetting

Grant and Middleman (1966, fig. 1), McCarthy and Molloy (1974, fig. 2), Dumouchel (2008, fig. 1), and Lefebvre and McDonell (2017, fig. 2.13) suggest that the breakup length in the dripping regime increases considerably with velocity. This seems unlikely. While the breakup length has not been measured in the dripping regime to my knowledge, presumably it can be approximately decomposed into the distance required for the liquid to start necking and the

droplet diameter. Assuming that the nozzle is very thin, the simple theory of Tate (Clanet and Lasheras, 1999, p. 308) suggests that approximately

$$D \propto \left(\frac{\sigma d_0}{\rho_\ell g} \right)^{1/3}. \tag{10}$$

If $\langle x_\mathrm{b} \rangle \propto D$ in the dripping regime, consistent with the idea that the necking distance is proportional to the droplet diameter, then we might expect

$$\frac{\langle x_\mathrm{b} \rangle}{d_0} \propto \left(\frac{\sigma}{\rho_\ell g d_0^2} \right)^{1/3} = \left(\frac{\mathrm{Fr}_0}{\mathrm{We}_{\ell 0}} \right)^{1/3}, \tag{11}$$

which does not vary with jet bulk velocity, $\overline{U}_0$. Now, it is possible that other effects will change this result, but likely the breakup length varies little with the jet bulk velocity in the dripping regime.

Existing dripping studies had laminar flows at the nozzle outlet, but it may be possible for a turbulent dripping state to also exist. Consequently, I marked a hypothesized turbulent dripping regime in the regime diagram developed in this work (figure 4), though I am unaware of any observations of this regime. Computation suggests a very large nozzle on the order of 4 inches in diameter is needed to observe turbulent dripping.

The transition from dripping to "jetting" (laminar Rayleigh regime) has been studied extensively in the literature. Clanet and Lasheras (1999) develop the following regime boundary for the end of dripping based on their theory and validate it with an extensive series of experiments:

$$\mathrm{We}_{\ell 0,\mathrm{crit}} = 4 \frac{\mathrm{Bo}_\mathrm{outer}}{\mathrm{Bo}} \left[1 + K \mathrm{BoBo}_\mathrm{outer} - ((1 + K \mathrm{BoBo}_\mathrm{outer})^2 - 1)^{1/2} \right]^2, \tag{12}$$

where $\mathrm{Bo}^2 \equiv \rho_\ell g d_0^2 / (2\sigma)$ and $\mathrm{Bo}_\mathrm{outer}^2 \equiv \rho_\ell g d_\mathrm{outer}^2 / (2\sigma)$ define the Bond numbers for the inside and outside of the nozzle orifice (d_outer is the outer diameter of the nozzle orifice), respectively, and K is a constant which equals 0.37 for water injected into air.

4.4 Laminar Rayleigh regime

A jet in the laminar Rayleigh regime is shown in figure 9. The theory of Weber (2019) accurately describes the breakup of jets in this regime. The equation for the breakup length in Weber's theory is

$$\frac{\langle x_\mathrm{b} \rangle}{d_0} = \ln \left(\frac{d_0}{2\delta_0} \right) \left(\mathrm{We}_{\ell 0}^{1/2} + 3 \frac{\mathrm{We}_{\ell 0}}{\mathrm{Re}_{\ell 0}} \right). \tag{13}$$

Based on limited data from Haenlein (1932), Weber (2019, p. 24) recommends $\ln(d_0/(2\delta_0)) = 12$ for the laminar Rayleigh regime. Grant and Middleman (1966, p. 673L) state that $\ln(d_0/(2\delta_0)) = 13.4$ fits their data better. Grant and Middleman further suggest that $\ln(d_0/(2\delta_0))$ is a function of $\mathrm{Oh}_{\ell 0}$. However, Kroesser and Middleman (1969, p. 385L) note that the variation in $\ln(d_0/(2\delta_0))$ as a function of $\mathrm{Oh}_{\ell 0}$ is "so weak that it probably does not warrant detailed investigation", suggesting that $\ln(d_0/(2\delta_0)) = 13.4$ is perfectly acceptable for engineering use.

4.5 Transition to the laminar non-Rayleigh regime

The laminar non-Rayleigh regime is not a major focus in this work, however, the studies of Leroux et al. (1996, 1997) (summarized by Dumouchel (2008, pp. 377–379)) can approximately

explain many of the recognized trends. For the regime diagrams in this work, the boundary line is approximated as $\mathrm{Re}_{\ell 0,\mathrm{crit}} \propto \mathrm{We}_{\ell 0}^{-1/2}$. This equation is motivated by a high Weber number approximation to a regression made by Reitz (1978, p. 24) to numerical calculations of the regime boundary by Sterling and Sleicher (1975, fig. 13). This regression is

$$\mathrm{We}_{\mathrm{g0,crit}} = 1.2 + 3.41\mathrm{Oh}_{\ell 0}^{0.9}, \tag{14}$$

which, at high $\mathrm{We}_{\ell 0}$ can be written as $\mathrm{Re}_{\ell 0,\mathrm{crit}} \propto \mathrm{We}_{\ell 0}^{-0.57}$. Given the uncertainties in this result, $\mathrm{Re}_{\ell 0,\mathrm{crit}} \propto \mathrm{We}_{\ell 0}^{-1/2}$ was deemed as a reasonable approximation.

4.6 Laminar non-Rayleigh regime

The defining visual characteristic of the laminar non-Rayleigh regime in this work is the flow (or at least the free surface) being laminar at the nozzle outlet, transitioning to turbulence downstream. The defining objective characteristic for the laminar non-Rayleigh regime is the breakup length decreasing as the velocity increases. All photographs with breakup length data in the data compilation are consistent with these definitions. While future work is needed, to the best of my knowledge downstream transition to turbulence coincides with the decrease in the breakup length. The cause of this transition could be any number of things discussed in the literature: the typical (single phase) causes of turbulence transition (including the velocity profile) or aerodynamic effects (Dumouchel, 2008; Leroux et al., 1996; and Trettel, 2019). Another possibility is that the boundary layer is laminar but the core of the flow is turbulent. Then, the spread of the turbulent region to the free surface can cause an apparent transition. Pipe jets, studied in this work, will not show this behavior as it typically occurs in a converging nozzle.

One non-obvious consequence of this categorization is that apparently none of the data of von Ohnesorge (again, who made the earliest regime diagram) is strictly in the turbulent surface breakup or atomization regimes now. Describing breakup at the highest velocities tested, von Ohnesorge (2019, p. 4) states (translated into English) "The atomization process III starts suddenly. The jet shows a smooth surface in the immediate vicinity of the nozzle outlet with axisymmetric swellings, which degenerate into helical transverse displacements of increasing amplitude." Presumably the "smooth surface" refers to an initially laminar flow. The photos provided in the journal article lack the resolution to show that the jet was initially laminar, so we only have von Ohnesorge's word that the jet was initially laminar. Some recent DNS studies may confirm that the flow at the outlet of a fuel spray nozzle (presumably like the nozzle von Ohnesorge used) is laminar (Agarwal and Trujillo, 2018 and Trujillo et al., 2018), however, this could be an artifact of not specifying turbulent inflow boundary conditions, as neither paper discusses whether turbulence was injected into the computational domain at the inflows.

Note that just because the flow is initially laminar does not mean that the breakup is not vigorous. On the contrary, as Hoyt and Taylor (1985) note, liquid jet flows which are initially laminar but transition downstream can have particularly vigorous breakup. Causing the flow to be turbulent at the nozzle outlet has been observed to greatly reduce the amount of breakup, as will be discussed in the next section. I propose that the "laminar non-Rayleigh regime" is actually a class of regimes. One of these regimes is like the Rayleigh regime (see figure 10), another is like the turbulent surface breakup regime (see figure 12), and another is like the atomization regime (see figure 11)[†]. The turbulent surface breakup and atomization regimes as defined in this work

[†]It is possible that the breakup observed in figure 11 is entirely independent of aerodynamic effects, which

could be viewed as merely fully turbulent versions of those regimes, while their corresponding regimes in the laminar non-Rayleigh class are merely transitional versions.

Unfortunately, because pipe nozzles have low critical Reynolds numbers, the laminar non-Rayleigh part of the $\mathrm{We}_{\ell 0}$–$\mathrm{Re}_{\ell 0}$ parameter space as seen in figure 5 is too small to easily distinguish between the different varieties of laminar non-Rayleigh breakup. Studies into the laminar non-Rayleigh regime in the future should use nozzles with higher critical Reynolds numbers for this reason.

The breakup length model used for the laminar non-Rayleigh regime in figures 6 and 8 is

$$\frac{\langle x_\mathrm{b} \rangle}{d_0} \propto \mathrm{We}_{\ell 0}^{-1}, \tag{15}$$

with the constant of proportionality chosen by setting the breakup length of the laminar Rayleigh regime equal to equation 15 at the transition point. This model is simple and motivated by the observation of Etzold et al. (2018) that at least sometimes in the laminar non-Rayleigh regime, $\langle x_\mathrm{b} \rangle \propto \overline{U}_0^{-2}$.

In principle it may be reasonable to model the laminar non-Rayleigh regime as follows: Model the turbulent-laminar transition by adding a transition length x_trans to all spatial locations and then using a model for whichever regime is relevant after the transition. However, the transition length is typically not known a-priori. The turbulence intensity when the flow starts being turbulent possibly could be calculated through a model similar to one I recently developed (Trettel, 2019). Presumably the turbulence intensity increases dramatically as the velocity increases in the laminar non-Rayleigh regime.

4.7 Transition to turbulence inside the nozzle

Depending on the location in the regime diagram, once transition is complete, transition to turbulence could decrease the breakup length (e.g., figure 7, transition from laminar to turbulent Rayleigh (Mansour and Chigier, 1994, fig. 5)), or increase it (e.g., figures 6 and 8, transition from laminar non-Rayleigh to turbulent surface breakup or atomization (Hoyt and Taylor, 1985)). The latter is because the laminar non-Rayleigh (i.e., external transition) regime can be particularly unstable (Trettel, 2019), as seen through it's decreasing breakup length with velocity. Hoyt and Taylor (1985) recommended if one wants a more stable jet to bring turbulence transition inside of the nozzle if it is occurring outside of the nozzle, which seems counterintuitive if you believe that earlier transition is bad, but one way to rephrase this recommendation is to avoid the laminar non-Rayleigh regime if one wants a stable jet. Even the atomization regime would be preferable in terms of breakup length.

4.8 Turbulent Rayleigh regime

As stated earlier, the turbulent Rayleigh regime appears similar to the Rayleigh regime, except that the jet is now turbulent at the nozzle outlet. A photo of a jet in the turbulent Rayleigh regime is shown in figure 13. Compared against the laminar Rayleigh regime, the breakup in the turbulent Rayleigh regime is less regular, but large droplets are still being produced downstream

would make the mechanism different than atomization, or possibly there are multiple types of this vigorous breakup, some of which have aerodynamic influence and others which do not.

like in the laminar Rayleigh regime. The turbulent Rayleigh regime follows Weber's theory for the breakup length:

$$\frac{\langle x_\mathrm{b}\rangle}{d_0} = \ln\left(\frac{d_0}{2\delta_0}\right)\left(\mathrm{We}_{\ell 0}^{1/2} + 3\frac{\mathrm{We}_{\ell 0}}{\mathrm{Re}_{\ell 0}}\right). \tag{13}$$

However, the initial disturbance level (δ_0/d_0) is higher than in the laminar case. Unfortunately the available data has little variation in turbulence intensity, so it is not possible to understand how the initial disturbance level varies with the turbulence level. The pipe nozzle data from Phinney (1973, 1975) and Sallam et al. (2002) appears to be consistent. Phinney (1975, p. 998R) suggests that $\ln(d_0/(2\delta_0)) = 3.27$ based on his data. However, van de Sande and Smith (1976, p. 221L) found that $\ln(d_0/(2\delta_0)) \approx 4.0$ and Mansour and Chigier (1994, pp. 597–598) found that $\ln(d_0/(2\delta_0)) \approx 4.8$ for jets in the turbulent Rayleigh regime. The turbulent Rayleigh regime is little studied and has hardly been recognized in previous work, so perhaps future work will clarify the source of these inconsistencies. It's possible a difference in turbulence intensity accounts for some of the inconsistency.

4.9 Transition from the turbulent Rayleigh regime to the turbulent surface breakup regime

The transition from the turbulent Rayleigh regime to the turbulent surface breakup regime is gradual, as both the Rayleigh (core breakup) and turbulent surface breakup mechanisms are present in both regimes. The difference is that the Rayleigh mechanism is dominant in the turbulent Rayleigh regime, and correspondingly, the turbulent surface breakup mechanism is dominant in the turbulent surface breakup regime. One simple way to measure the relative strengths of each mechanism would be to compute the ratio of the average breakup onset location, $\langle x_\mathrm{i}\rangle$, to the average breakup length in the turbulent Rayleigh regime, $\langle x_\mathrm{b}\rangle$[‡]. In the turbulent Rayleigh regime, presumably a long distance is needed for turbulent surface breakup to start, hence, $\langle x_\mathrm{i}\rangle \gg \langle x_\mathrm{b}\rangle$. The opposite is true in the turbulent surface breakup regime. Using the average breakup onset location theory developed by Trettel (2020a) and Weber's breakup length theory (equation 13)

$$\frac{\langle x_\mathrm{i}\rangle}{\langle x_\mathrm{b}\rangle} \propto \frac{\overline{\mathrm{Tu}_0}^{-3}\mathrm{We}_{\ell 0}^{-1}}{\ln\left(\frac{d_0}{2\delta_0}\right)\left(\mathrm{We}_{\ell 0}^{1/2} + 3\frac{\mathrm{We}_{\ell 0}}{\mathrm{Re}_{\ell 0}}\right)} \equiv \frac{1}{C_{\text{TR to TSB}}}. \tag{16}$$

The transition between the two regimes is defined here as a certain critical value of the ratio $\langle x_\mathrm{i}\rangle/\langle x_\mathrm{b}\rangle$. Rearranging this ratio returns

$$\frac{C_{\text{TR to TSB}}\overline{\mathrm{Tu}_0}^{-3}}{\ln\left(\frac{d_0}{2\delta_0}\right)} = \mathrm{We}_{\ell 0,\text{crit}}^{3/2} + 3\frac{\mathrm{We}_{\ell 0,\text{crit}}^2}{\mathrm{Re}_{\ell 0}}, \tag{17}$$

[‡]Equating the expressions for the breakup length in each regime is another possibility, however, as there currently no good theory for the turbulent surface breakup regime's breakup length but there is for the breakup onset location, the latter was deemed a better choice. I view the atomization regime boundary in § 4.11 found through equating empirical expressions for breakup length at tentative at best. Using validated theoretical expressions instead of simple power law regressions and then equating those would be better, and I am trying to get closer to that ideal in the boundary between the turbulent Rayleigh regime and the turbulent surface breakup regime.

where the Weber number has been labeled as the critical Weber number. Equation 17 is an implicit algebraic equation for $\mathrm{We}_{\ell 0,\mathrm{crit}}$.

The high Reynolds number limit of $\mathrm{We}_{\ell 0,\mathrm{crit}}$ is easily found:

$$\mathrm{We}_{\ell 0,\mathrm{crit},\infty} = \frac{C_{\text{TR to TSB}}^{2/3} \overline{\mathrm{Tu}_0}^{-2}}{\ln\left(\frac{d_0}{2\delta_0}\right)^{2/3}}. \tag{18}$$

If $\ln(d_0/(2\delta_0))$ is assumed constant, then the equation

$$\mathrm{We}_{\ell 0,\mathrm{crit},\infty} = 8\overline{\mathrm{Tu}_0}^{-2} \tag{19}$$

fits the limited available data.

4.10 Turbulent surface breakup regime

Breakup in the turbulent surface breakup regime is caused primarily by turbulent fluctuations perforating the free surface (Trettel, 2020a). Figure 14 shows what a jet in the turbulent surface breakup regime looks like near the nozzle. The breakup here is rather vigorous, but it is limited to the free surface of the jet rather than the core itself as in the turbulent Rayleigh regime. Farther downstream, as shown in figure 15, the jet core may fragment, but in a much more disordered way than seen in the turbulent Rayleigh regime.

A variety of regressions were developed for the turbulent surface breakup regime in this work. The database is described in detail in Trettel (2020b). The most important, the breakup length regression, made use of data from Kusui (1969) with significant turbulence intensity variation ($5.4\% \leq \overline{\mathrm{Tu}_0} \leq 12.7\%$). This regression is (194 points, $R^2 = 0.959$):

$$\frac{\langle x_\mathrm{b} \rangle}{d_0} = 3.61\overline{\mathrm{Tu}_0}^{-0.275}\mathrm{We}_{\ell 0}^{0.334}. \tag{20}$$

A regression was made for the spray angle in the turbulent surface breakup regime. Unfortunately, the spray angle data of Skrebkov (1966) with turbulence intensity variation is in the atomization regime (according to equation 26), so it is not possible to determine the sensitivity to the turbulence intensity for the spray angle in the turbulent surface breakup regime at the moment. Analysis of available data in either the turbulent surface breakup or atomization regimes suggests that the available spray angle data is far too noisy to use for regression purposes. This is likely due to the lack of standard definitions of the spray angle — see Trettel (2020b) for a discussion of this problem. Using only data from the Faeth group (Ruff (1990) and Sallam (2002)), which appears to be less noisy and may have used a consistent definition, returns (5 points, $R^2 = 0.989$):

$$\tan\left(\frac{\theta_\mathrm{i}}{2}\right) = 5.32 \times 10^{-5}\mathrm{We}_{\ell 0}^{0.605}. \tag{21}$$

Similarly, because there is no data meeting the guidelines described in Trettel (2020b) with appreciable turbulence intensity variation for $\langle x_\mathrm{i} \rangle$, D_{32}, or $\langle v_\mathrm{d} \rangle$, a regression analysis was done using composite variables including both the Weber number and the turbulence intensity as the

theory in Trettel (2020a) predicted they'll appear. For the breakup onset location, the regression is (52 points, $R^2 = 0.758$)

$$\frac{\langle x_\mathrm{i} \rangle}{d_0} = 13.0 \left(\overline{\mathrm{Tu}_0}^3 \mathrm{We}_{\ell 0} \right)^{-0.915}. \tag{22}$$

For the Sauter mean diameter, only data at the breakup onset location had known turbulence intensities, so only data there was used in the regression. The regression equation is (23 points, $R^2 = 0.752$)

$$\frac{D_{32}}{d_0} = 0.649 \left(\overline{\mathrm{Tu}_0}^2 \mathrm{We}_{\ell 0} \right)^{-0.657}. \tag{23}$$

And like the Sauter mean diameter, for the radial droplet velocity after formation, only data at the breakup onset location had known turbulence intensities. As such, the regression equation is (17 points, $R^2 = -0.0131$)

$$\frac{\langle v_\mathrm{d} \rangle}{\overline{v_0'}} = 0.0582 \left(\overline{\mathrm{Tu}_0}^2 \mathrm{We}_{\ell 0} \right)^{0.0322}. \tag{24}$$

Some additional discussion of these regressions is in Trettel (2020a).

4.11 Atomization regime and the transition from the turbulent surface breakup regime

A variety of mechanisms are factors in the atomization regime: turbulence, shear/atmospheric effects (density ratio), cavitation, and Mach number effects. A near-nozzle photo of a jet likely in the atomization regime is in figure 16. A downstream photo is in figure 17. Note how the atomization regime is superficially similar to the turbulent surface breakup regime as shown in figure 14. This highlights the need for objective characteristics defining the atomization regime, in this case using the breakup length. Here I'll define the atomization as a regime where the power law increase of the breakup length no longer applies.

Drawing a line in a regime diagram to get the boundary equation direcetly does not seem prudent as the data is relatively sparse at high Weber and Reynolds numbers. Instead, I'll note that at low Mach numbers, the breakup length appears to plateau in the data of Kusui (1969) and Sallam (2002) in the atomization regime. In other words, the breakup length is an increasing power law in $\mathrm{We}_{\ell 0}$ for the turbulent surface breakup regime, but once the jet enters the atomization regime, the breakup length plateaus. In this case, finding the intersection of breakup length correlations for the turbulent surface breakup and atomization regimes would return an equation for the boundary of the two regimes.

Unfortunately, if one limits the analysis to the available low Mach number ($\mathrm{Ma}_\mathrm{g} < 0.3$) data for pipe jets, one can not distinguish between cavitation and the density ratio. The cases with low $\rho_\ell/\rho_\mathrm{g}$ also have only sudden contraction entrances to the pipe, while the cases with high $\rho_\ell/\rho_\mathrm{g}$ have only smooth entrances to the pipe. Sudden contractions are more prone to cavitation (Ahn et al., 2006, fig. 3), which reduces the breakup length, just like low density ratios. Problems like this are called "confounding" and is discussed more in Trettel (2020b).

Regressing the available data, shortcomings and all, results in the following equation for the breakup length in the atomization regime (11 points, $R^2 = 0.602$, $\rho_\ell/\rho_\mathrm{g}$ ranging from 29.4 to 882):

$$\frac{\langle x_\mathrm{b} \rangle}{d_0} = 5.31 \overline{\mathrm{Tu}_0}^{-0.568} \left(\frac{\rho_\ell}{\rho_\mathrm{g}} \right)^{0.335}, \tag{25}$$

which implies the following turbulent surface breakup to atomization regime boundary:

$$\mathrm{We}_{\ell 0,\mathrm{crit}} = 3.17\overline{\mathrm{Tu}_0}^{-0.876}\left(\frac{\rho_\ell}{\rho_\mathrm{g}}\right)^{1.00}. \tag{26}$$

The density ratio exponent given above is accurate to 3 significant figures — it does not equal 1 exactly here. Note that equation 26 approximates a simple critical gas Weber number criteria:

$$\mathrm{We}_{\mathrm{g}0,\mathrm{crit}} = 3.17\overline{\mathrm{Tu}_0}^{-0.876}. \tag{27}$$

The use of a critical gas Weber number for atomization as suggested by Reitz (1978, p. 8) and discussed in § 3.2 appears reasonable given the limited amount of data available. And, the critical gas Weber number predicted by equation 26 for 5% turbulence and a density ratio of $1000/1.2$ (approximating water and air) is 44.8, not far from the number 40.3 Reitz suggested in error. The simplest explanation for why Reitz's criteria ends up being accurate despite the miscalculation is coincidence combined with the fact that the data the criteria was based on did not look at objective characteristics like the breakup length. It likely corresponded to a different boundary, assuming it was not entirely spurious.

As shown in figure 5, equation 26 appears to be conservative in terms of putting more data in error in the turbulent surface breakup regime than in the atomization regime.

5. CONCLUSIONS

Liquid jets break up in 6 regimes recognized in this work: dripping, laminar Rayleigh, laminar non-Rayleigh, turbulent Rayleigh, turbulent surface breakup, and atomization. The turbulent Rayleigh regime has rarely been recognized due to the common but erroneous belief that as the velocity of a jet increases the jet first starts dripping, then enters the (conventionally laminar) Rayleigh regime, then enters the laminar non-Rayleigh regime, then enters the turbulent surface breakup regime, and then enters the atomization regime. This regime progression was shown to be only one of several possibilities. Particularly small jets (or equivalently, particularly viscous jets) may never enter the turbulent surface breakup regime and skip from laminar non-Rayleigh to atomization. Similarly, particularly large jets (or equivalently, particularly non-viscous jets) may never enter the laminar non-Rayleigh regime and instead enter the turbulent Rayleigh regime prior to the turbulent surface breakup regime.

The regime of a jet is typically determined through subjective comparison against prototypical photographs of jets. This procedure was shown to be ambiguous, and instead regime classification based on objective characteristics like the breakup length was proposed.

The critical Reynolds number for the onset of turbulence at the nozzle outlet is a factor typically neglected in regime diagrams. The critical Reynolds number can vary by roughly two orders of magnitude in practice, and whether the jet is turbulent or laminar at the nozzle outlet can strongly influence how the jet breaks up.

The laminar non-Rayleigh regime itself appears to contain multiple other regimes similar to the turbulent surface breakup and atomization regimes, however, the available data makes studying the boundaries inside of the laminar non-Rayleigh regime difficult. This is due to the low critical Reynolds number in the data used in this study, which made the area in the $\mathrm{We}_{\ell 0}$-$\mathrm{Re}_{\ell 0}$ parameter space covered by the laminar non-Rayleigh regime too small to map the regime.

The popular Ohnesorge diagram (figure 2) is inaccurate and should not be used. A *schematic* diagram (figure 4) is proposed as a replacement, though it must be emphasized that this diagram

is merely a schematic which applies only for a special case. More general equations for the boundaries of each regime were given that can be used to determine the regime in more general cases.

REFERENCES

Agarwal, A. and Trujillo, M.F., A Closer Look at Linear Stability Theory in Modeling Spray Atomization, *International Journal of Multiphase Flow*, vol. **109**, pp. 1–13, 2018.

Ahn, K., Kim, J., and Yoon, Y., Effects of orifice internal flow on transverse injection into subsonic cross-flows: Cavitation and hydraulic flip, *Atomization and Sprays*, vol. **16**, no. 1, 2006.

Birouk, M. and Lekic, N., Liquid jet breakup in quiescent atmosphere: A review, *Atomization and Sprays*, vol. **19**, no. 6, pp. 501–528, 2009.

Chigier, N. and Reitz, R.D., 1996. Regimes of Jet Breakup and Breakup Mechanisms (Physical Aspects). *Recent Advances in Spray Combustion: Spray Atomization and Drop Burning Phenomena*. American Institute of Aeronautics and Astronautics, pp. 109–135.

Clanet, C. and Lasheras, J.C., Transition from dripping to jetting, *Journal of Fluid Mechanics*, vol. **383**, pp. 307–326, 1999.

Dumouchel, C., On the experimental investigation on primary atomization of liquid streams, *Experiments in Fluids*, vol. **45**, no. 3, pp. 371–422, 2008.

Eisenklam, P. and Hooper, P.C., Flow characteristics of laminar and turbulent jets of liquid, Report J.R.L. 42, Imperial College of Science and Technology, London, UK, 1958.

Etzold, M., Deswal, A., Chen, L., and Durst, F., Break-up length of liquid jets produced by short nozzles, *International Journal of Multiphase Flow*, vol. **99**, pp. 397–407, 2018.

Faeth, G.M., Structure and atomization properties of dense turbulent sprays, *Symposium (International) on Combustion*, vol. **23**, no. 1, pp. 1345–1352, 1991.

Grant, R.P., Newtonian Jet Stability, PhD dissertation, University of Rochester, Rochester, NY, 1965.

Grant, R.P. and Middleman, S., Newtonian jet stability, *AIChE Journal*, vol. **12**, no. 4, pp. 669–678, 1966.

Haenlein, A., Disintegration of a Liquid Jet, Technical Memorandum 659, National Advisory Committee for Aeronautics, Washington, DC, 1932.

Hoyt, J.W. and Taylor, J.J., Waves on water jets, *Journal of Fluid Mechanics*, vol. **83**, no. 1, pp. 119–127, 1977.

Hoyt, J.W. and Taylor, J.J., Pipe-exit flow photography, *Cavitation and Polyphase Flow Forum — 1980*, ASME, New Orleans, LA, pp. 42–44, 1980.

Hoyt, J.W. and Taylor, J.J., Effect of nozzle boundary layer on water jets discharging in air, *Jets and Cavities: International Symposium*, Kim, J.H., Furuya, O., and Parkin, B.R. (Eds.), Vol. 31 of *FED*, ASME, Miami Beach, FL, pp. 93–100, 1985.

Kroesser, F.W. and Middleman, S., Viscoelastic jet stability, *AIChE Journal*, vol. **15**, no. 3, pp. 383–386, 1969.

Kusui, T., Liquid Jet Flow into Still Gas: Jet Flow by Circular Rough Tube, *Bulletin of JSME*, vol. **12**, no. 53, pp. 1062–1071, 1969.

Lebedev, O.N., On the issue of atomizing fuel with diesel injectors, Translation, University of Texas at Austin, 2019.

Lefebvre, A.H. and McDonell, V.G., *Atomization and Sprays*, 2nd Edition, CRC Press, Boca Raton, FL, 2017.

Leroux, S., Dumouchel, C., and Ledoux, M., The stability curve of Newtonian liquid jets, *Atomization and Sprays*, vol. **6**, no. 6, 1996.

Leroux, S., Dumouchel, C., and Ledoux, M., The Break-up Length of Laminar Cylindrical Liquid Jets. Modification of Weber's Theory, *International Journal of Fluid Mechanics Research*, vol. **24**, no. 1-3, 1997.

Lin, S.P. and Reitz, R.D., Drop and Spray Formation from a Liquid Jet, *Annual Review of Fluid Mechanics*, vol. **30**, no. 1, pp. 85–105, 1998.

Littaye, G., Contribution à l'étude des jets liquides [Contribution to the study of liquid jets], Publications scientifiques et techniques du Secrétariat d'etat à l'Aviation 181, Paris, France, 1942.

Littaye, G., On a theory for the pulverisation of liquid jets [Review 45], *Bulletin, International Institute of Refrigeration*, vol. **25**, no. II, pp. 57–58, 1944.

Magnotti, G.M., Modeling the Influence of Nozzle-Generated Turbulence on Diesel Sprays, PhD dissertation, Georgia Institute of Technology, Atlanta, GA, 2017.

Mansour, A. and Chigier, N., Effect of turbulence on the stability of liquid jets and the resulting droplet size distribution, *Atomization and Sprays*, vol. **4**, no. 5, pp. 583–604, 1994.

McCarthy, M.J. and Molloy, N.A., Review of stability of liquid jets and the influence of nozzle design, *The Chemical Engineering Journal*, vol. **7**, no. 1, pp. 1–20, 1974.

Miesse, C.C., Correlation of Experimental Data on the Disintegration of Liquid Jets, *Industrial & Engineering Chemistry*, vol. **47**, no. 9, pp. 1690–1701, 1955.

Mullin, T., Experimental Studies of Transition to Turbulence in a Pipe, *Annual Review of Fluid Mechanics*, vol. **43**, no. 1, pp. 1–24, 2011.

Pfenniger, W., 1961. Transition in the inlet length of tubes at high Reynolds numbers, *Boundary Layer and Flow Control*. Lachmann, G.V. (Ed.). Pergamon, New York, NY, pp. 970–980.

Phinney, R.E., The breakup of a turbulent liquid jet in a gaseous atmosphere, *Journal of Fluid Mechanics*, vol. **60**, no. 4, pp. 689–701, 1973.

Phinney, R.E., Breakup of a turbulent liquid jet in a low-pressure atmosphere, *AIChE Journal*, vol. **21**, no. 5, pp. 996–999, 1975.

Portillo, J.E., Collicott, S.H., and Blaisdell, G.A., Measurements of axial instability waves in the near exit region of a high speed liquid jet, *Physics of Fluids*, vol. **23**, no. 12, p. 124105, 2011.

Ranz, W.E., *On Sprays and Spraying; a Survey of Spray Technology for Research and Development Engineers*, no. 65 in Bulletin, Pennsylvania State University, Department of Engineering Research, University Park, PA, 1956.

Reitz, R.D., Atomization and Other Breakup Regimes of a Liquid Jet, PhD dissertation, Princeton University, Princeton, NJ, 1978.

Reitz, R.D. and Bracco, F.V., 1986. Mechanisms of breakup of round liquid jets. *Encyclopedia of Fluid Mechanics*. Vol. 3. Gulf Pub. Co., Book Division, Houston, TX, pp. 233–249.

Ruff, G.A., Structure and Mixing Properties of the Near-Injector Region of Nonevaporating Pressure-Atomized Sprays, PhD dissertation, University of Michigan, Ann Arbor, MI, 1990.

Rupe, J.H., On the dynamic characteristics of free-liquid jets and a partial correlation with orifice geometry, Technical Report 32-207, Jet Propulsion Laboratory, Pasadena, CA, 1962.

Sallam, K.A., Properties of Spray Formation by Turbulent Primary Breakup, PhD dissertation, University of Michigan, Ann Arbor, MI, 2002.

Sallam, K.A., Dai, Z., and Faeth, G.M., Liquid breakup at the surface of turbulent round liquid jets in still gases, *International Journal of Multiphase Flow*, vol. **28**, no. 3, pp. 427–449, 2002.

Schillaci, E., Antepara, O., Balcázar, N., Serrano, J.R., and Oliva, A., A numerical study of liquid atomization regimes by means of conservative level-set simulations, *Computers & Fluids*, vol. **179**, pp. 137–149, 2019.

Skrebkov, G.P., Turbulent Pulsations in a Liquid Jet, and Its Atomization, *Journal of Applied Mechanics and Technical Physics (Foreign Technology Division)*, no. 3, pp. 142–151, 1966.

Sterling, A.M. and Sleicher, C.A., The instability of capillary jets, *Journal of Fluid Mechanics*, vol. **68**, no. 3, pp. 477–495, 1975.

Tafreshi, H.V. and Pourdeyhimi, B., The effects of nozzle geometry on waterjet breakup at high Reynolds numbers, *Experiments in Fluids*, vol. **35**, no. 4, pp. 364–371, 2003.

Tang, L. and Masutani, S.M., Laminar to Turbulent Flow Liquid-liquid Jet Instability and Breakup, *The Thirteenth International Offshore and Polar Engineering Conference*, International Society of Offshore and Polar Engineers, pp. 317–324, 2003.

Tate, T., On the magnitude of a drop of liquid formed under different circumstances, *The London, Edinburgh, and Dublin Philosophical Magazine and Journal of Science*, vol. **27**, no. 181, pp. 176–180, 1864.

Tonkonogiy, Y.L., Buz, V.N., Garbuz, A.A., and Kalinchak, A.I., Effect of roughness on the transition Reynolds number, *Fluid mechanics: Soviet research*, vol. **19**, no. 4, pp. 13–19, 1990.

Torda, T.P., Evaporation of drops and breakup of sprays, *Astronautica Acta*, vol. **18**, pp. 383–393, 1973.

Trettel, B., Turbulent theory of velocity-profile-induced jet breakup, *ILASS-Americas 2019*, Owkes, M. (Ed.), Tempe, AZ, 2019, Paper no. 19.

Trettel, B., Conditional damped random surface velocity theory of turbulent jet breakup, *Atomization and Sprays*, 2020a, (To be submitted.).

Trettel, B., Improving the validation of turbulent jet breakup models, *Atomization and Sprays*, 2020b, (To be submitted.).

Trujillo, M.F., Gurjar, S., Mason, M., and Agarwal, A., Global characterization of the spray formation process, *Atomization and Sprays*, vol. **28**, no. 9, 2018.

van de Sande, E. and Smith, J.M., Jet break-up and air entrainment by low velocity turbulent water jets, *Chemical Engineering Science*, vol. **31**, no. 3, pp. 219–224, 1976.

von Ohnesorge, W., Die Bildung von Tropfen an Düsen und die Auflösung flüssiger Strahlen [The formation of drops by nozzles and the breakup of liquid jets], *Zeitschrift für Angewandte Mathematik und Mechanik*, vol. **16**, no. 6, pp. 355–358, 1936.

von Ohnesorge, W., The formation of drops by nozzles and the breakup of liquid jets, Translation, University of Texas at Austin, 2019.

Weber, C., Breakup of a liquid jet, Translation, University of Texas at Austin, 2019.

Wu, P.K., Liquid Surface Breakup of Nonturbulent and Turbulent Liquids, PhD dissertation, University of Michigan, Ann Arbor, MI, 1992.

Wu, P.K. and Faeth, G.M., Aerodynamic effects on primary breakup of turbulent liquids, *Atomization and Sprays*, vol. **3**, no. 3, pp. 265–289, 1993.

Wu, P.K., Miranda, R.F., and Faeth, G.M., Effects of initial flow conditions on primary breakup of nonturbulent and turbulent round liquid jets, *Atomization and Sprays*, vol. **5**, no. 2, pp. 175–196, 1995.